

## **UNPROTECTED TIMBER- FIBRE REINFORCED CONCRETE SLAB IN FIRE**

LUKÁŠ BLESÁK, EVA CALDOVÁ, FRANTIŠEK WALD  
CZECH TECHNICAL UNIVERSITY IN PRAGUE  
DEPARTMENT OF STEEL AND TIMBER STRUCTURES  
PRAGUE, CZECH REPUBLIC

(RECEIVED APRIL 2015)

### **ABSTRACT**

Combining structural materials, so their beneficial mechanical properties are utilized in the very best way, represents an effective way how to progress in the building industry nowadays. Coupled timber-concrete structures are well known in the civil engineering and have been applied in practise for decades. Following the fire safety requirements, there are many ongoing projects aiming to understand the behaviour of such structures exposed to elevated temperatures. Several real-size experiments have been performed under a supervision of Czech Technical University in Prague (Bednář et al. 2013, Caldová et al. 2014 b). The main goal of this paper is to present a benchmark on a final element model of such a structure focusing on the input data application and a description of the subjected structure behaviour exposed to high temperatures.

**KEYWORDS:** Glued laminated timber, fibre concrete, fire, numerical simulation.

### **INTRODUCTION**

Besides the beneficial properties of timber including mainly the ecological and structural factors, timber is also well known for its high mechanical performance in relation to its bulk density. Combination of this natural resource with other semi-artificial structural materials, such as steel, concrete or glass enables using timber in the very best way, whilst its weak mechanical and physical properties are covered by the other materials used and vice versa. Building industry and its rapid development requires new technologies, structural procedures and gadget solutions preceded and followed by new requirements and standard regulations. The ongoing research partially described in this paper focuses on fire resistance of the presented timber-fibre concrete slab structure taking its deflections and overall integrity into account.

Fibre concrete has not been developed recently; however, its various mixtures and additives are still being developed and tested. Plain concrete reinforced by steel fibres and also filled with polymer fibres dispose of better mechanical properties, such as higher tension strength

– approximately two to three fold comparing to parent plain concrete – depending on various factors, such as the parent concrete strength class and type and volume content of steel fibres. Fibre concrete is a ductile material and resists tension stresses even in the post-crack action. Polymer fibres content contributes in higher resistance of fibre concrete mixture in spalling in elevated temperatures, as the water evaporation and consequent internal pressure is decreased due to polymer fibres being burned out. For a detailed description of SFRC behaviour in both elevated and ambient temperatures see paper (Blesák et al. 2015).

One of the very beneficial advantages of a coupled fibre-concrete load-bearing system is not only its low dead-weight but even its fire resistance, which is mainly influenced by the timber used – timber cross-section dimensions, timber density and so its charring rate, the coupling system properties and the fibre concrete mixture as well.

The main goal of the real-size experiment presented in this paper is to investigate the fire resistance of timber-concrete ceiling slab with the internal-span beams thermal uninsulated. Timber disposes of self-protect ability when exposed to fire – average charring rate of timber is  $38 \text{ mm}\cdot\text{h}^{-1}$  by temperature  $t = 290^\circ\text{C}$ . Burning of timber can be divided into three phases: Initiation, propagation and heating (Reinprecht 2008). Following the surface thermal processes in a timber element, there are several layers characterized by various mechanical properties effecting the global cross-section's behaviour, whilst the mechanical properties of timber are considered to be decreased to zero when reaching temperature  $300^\circ\text{C}$  (ČSN EN 1995-1-2 2006). Charring rate  $0.5 \text{ mm}\cdot\text{min}^{-1}$  (ČSN EN 1995-1-2 2006) is taken into account in the frame of the presented research.

In this paper, a brief description of the real-size experiment and material tests are followed by a description of a numerical analysis taking the material non-linearity, geometric non-linearity, time and temperature dependence of material properties into account.

## MATERIAL AND METHODS

### Experimental set-up

Dimensions of the tested slab structure was opted based on the fire furnace dimensions – 3.5 by 4.0 m. The SFRC slab with thickness 60 mm was supported by a thermal isolated glued laminated timber frame with cross-sectional dimensions 200 x 240 mm and two internal beams with cross-sectional dimensions 100 x 160 mm placed in the thirds of a shorter span. All timber elements were made of material GL36c. Fibre concrete mixture was composed of parent concrete classified as 45/55 strength class, content of hooked end steel fibres HE 75/50 Arcelor was  $70 \text{ kg}\cdot\text{m}^{-3}$ , polypropylene fibres  $1.5 \text{ kg}\cdot\text{m}^{-3}$ . Timber-concrete coupling was ensured by screws TCC 7.3 x 150 mm inclined  $45^\circ$  and placed in a mutual distance 100 mm in two parallel rows. The specimen was loaded by mechanical loading represented by two concrete blocks placed on the slab by means of steel plates 200 x 200 mm in the thirds of the internal beam's span. Afterwards, the tested structure was loaded by the actions of nominal fire for 60 min. – fire curve ISO 834 2014. For the test set-up see Fig. 1. The test set-up details, number and location of measuring points and other necessary details are introduced in paper (Ekr et al. 2015).

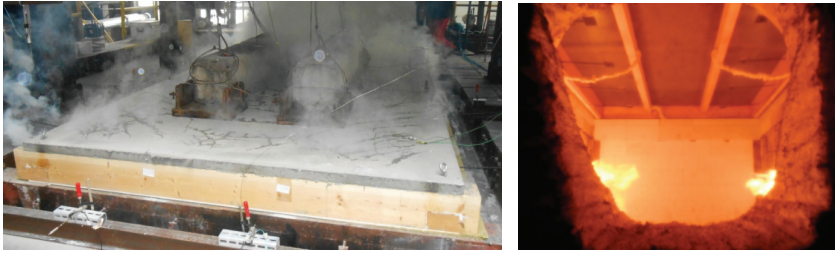


Fig. 1: Test set-up with mechanical loading applied during the fire exposure (left), view over the bottom edge of tested slab during the fire exposure (right).

### Material properties

For the purposes of numerical simulations, push-out test of timber-concrete coupling was performed (Caldova et al. 2014a), further, four point bending tests of SFRC prisms in both ambient and elevated temperature were performed (will be published later) and four point bending test of the used timber was performed too (Caldova et al. 2014a).

### Glued laminated timber

Resulting the performed material tests, Young's modulus of elasticity of timber GL36c at ambient temperature was considered as equal to 11.22 GPa for both the frame and beams material. As temperature increases, timber burns out – this fact was considered by applying an effective Young's modulus of elasticity, whilst its decrease was linear from its initial value down to 50 GPa. Taking a zero value into account would cause divergences in the numerical model. Young's modulus of elasticity of timber was controlled in time in, not as a function of temperature, which showed to be sufficient and proper for numerical purposes.

### Steel fibre reinforced concrete – SFRC

Based on the material tests performed on SFRC cubes and prisms, specific material properties for ambient temperature were defined as follows:

Young's modulus of elasticity:	$E = 48450 \text{ GPa}$
Poisson ration:	$\nu = 0.2$
Tension strength:	$f_t = 7.4 \text{ MPa}$
Compression strength:	$f_c = -80.9 \text{ MPa}$

Software Atena Science was used for the numerical simulation. This software was opted for its advanced settings of concrete-based materials and even a relevant fibre concrete simulation. Fracture energy  $G_f = 9000 \text{ N.m}^{-1}$  was defined in compliance with (Sajdlová 2011); crack opening law parameters and compression ductility parameters were specified following the ongoing research performed on ČVUT focused on defining the proper values of non-linear behaviour in both ambient and elevated temperatures. The results of the ongoing research will be published soon.

As there is not sufficient evidence of the specific values of fracture energy of various SFRC mixture, one of the ways how to define this is experimentally performing a uni-axial tension test. However, as this is rather a demanding procedure, the fracture energy may be defined also empirically or be derived following relevant literature, see e.g. (Salehian et al. 2014, Barros et al.

2001, Elsaigh 2001).

Multipliers of the basic SFRC material properties as a function of temperature are listed in Tab. 1. As the maximum temperature in fibre concrete resulting from a thermal analysis reached up to 850°C, the material properties were left constant after reaching this temperature. Values marked as “-“ were linear interpolated.

Tab. 1: Material properties of SFRC decreased in elevated temperature.

Temperature (°C)	0	100	200	300	400	500	600	700	800
E modulus	1	0.5938	0.4091	0.3036	0.1875	0.1	0.045	0.03	0.015
Tension strength $f_t$	1	1	-	-	-	0.2	0.01	-	0.01
Compression strength $f_c$	1	0.95	-	0.85	0.75	-	-	-	0.15
Onset of crushing $f_{c0}$	1	0.95	-	0.85	0.75	-	-	-	0.15
Fracture energy $G_f$	1	-	1	1.3	2	-	-	-	2
Thermal strain $\epsilon_T$ (x 10 <sup>-4</sup> )	0	7.43	18.04	31.41	48.92	71.95	101.88	140	140

### Timber-concrete coupling

Timber-concrete coupling stiffness was defined based on the results gained from the push-out test performed for the coupling system used in this experiment (Caldová et al. 2014b). Its behaviour was considered linear with the maximum slip movement  $\Delta_{\text{slip}} = 2.6$  mm when force  $F = 280$  kN. As the push-out test set-up presented in paper (Caldová et al. 2014a) is symmetrical, force  $F/2$  acts over the coupling system composed of  $6 \times 45^\circ$  inclined screws spaced 100 mm in the longitudinal direction placed in two parallel rows. Therefore, the tangential stiffness  $K_{TT}$  of the areal solid-solid interface of the timber-concrete coupling is defined following formula (1).

$$K_{TT} = \frac{\frac{F}{2}}{b \times \frac{n_s}{n_r} \times m_s} \left[ \frac{\text{MN}}{\text{m}^3} \right] \quad (1)$$

where:  $F$  - the force acting over the push-out test set-up,  
 $\Delta_{\text{slip}}$  - slip movement,  
 $b$  - beam width,  
 $n_s$  - number of screws in one half of the push-out test set-up,  
 $n_r$  - number of rows of screws,  
 $m_s$  - distance of screws in longitudinal direction,

$K_{TT,a}$  - (frame interface) = 900 MN.m<sup>-3</sup>,

$K_{TT,b}$  - (beam interface) = 1800 MN.m<sup>-3</sup>.

Decrease of the coupling tangential stiffness in elevated temperatures was not taken into account. The coupling is considered to be fire-protected by the beam before its failure and the reduction of concrete strength has a secondary effect over a coupling stiffness. The same is valid for concrete strength-class reduction and its effect over a coupling stiffness (Sandanus 2007).

### Numerical simulation

The overall numerical analysis is in principal based on the outputs of two analyses – thermal and static. In case of both, specific values were observed and compared with the ones resulting from real-size experiments. The input material parameters were taken from relevant standards, literature and the material tests performed for the purposes of this research. Element size was

opted taking the computational efficiency into account – computational time and results precision. For the slab, shell elements with thickness 20 mm and ground-plan dimensions 150 x 150 mm were applied; for the internal beam, four solid elements in height and two in width were applied. For 3D solid elements, maximal ration of sides dimensions from 1/3 to 1/4 was not exceeded.

### Thermal analysis

Thermal analysis was performed to gain the appropriate results as an input for the static analysis. Specific thermal properties were considered constant, defined as follows:

Coefficient defining heat flux:	SFRC: 1.70 W/(K.m)
	timber: 0.15 W/(K.m)
Coefficient defining heat material capacity:	SFRC: $4.5 \times 10^6$ J/(m <sup>3</sup> .K)
	timber: $0.1 \times 10^6$ J/(m <sup>3</sup> .K)

Thermal properties of timber were modified in compliance with (ČSN EN 1995-1-2 2006) and considered constant. Thermal properties of concrete were taken from (Wald et al. 2005) and consequently modified for the purpose of this simulation.

Fire curve ISO 834 2014 was used to fire-load the structure from the bottom edge, temperature on the top edge was defined to 25°C, the same as the initial temperature of all the used materials.

Convection heat transfer coefficient was considered 50 W/(°C.m<sup>2</sup>), resulting emissivity factor of the radiation source and heat transfer 0.7 (Wald et al. 2005).

The proper values of temperature across the slab thickness are essential not only because of the fibre concrete material properties being decreased based on temperature, but also due to thermal deformation of the subjected structural system. Temperature of SFRC slab was measured by 14 thermo-couples concreted 20 and 40 mm above the bottom edge located in 5 places in the slab. Temperature on the cool surface was measured too. Average values of the measured values and the values gained from the analysis are summarized in Fig. 2.

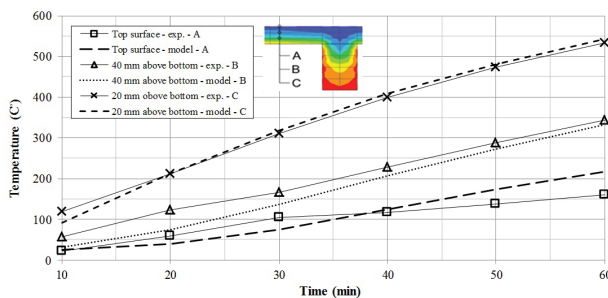


Fig. 2: Experimental and simulated values of temperature across the slab thickness.

As the thermal gradient across the slab thickness is non-linear, three layers of shell elements placed one on another were used in the numerical simulation. Thermal data are transported into the static calculation considering the surface points of the shell elements, therefore using just one shell element across the slab thickness would lead to misleading thermal gradient pattern, see Fig. 3.

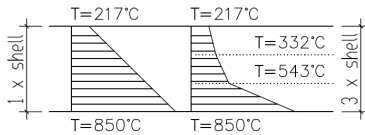


Fig. 3: Thermal gradient pattern across the slab thickness in 60 min. – 1 x shell element (left) vs. 3 x shell elements (right) across the slab thickness.

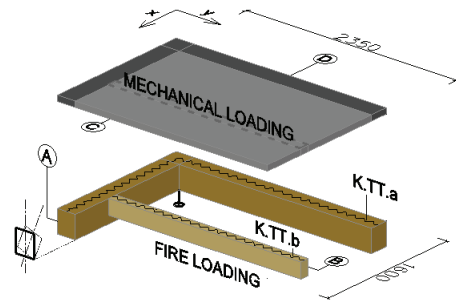


Fig. 4: Scheme of the numerical model.

## Static analysis

### Static scheme and loading

Geometry related to the real-size experiment was applied in the static analysis. The overall ground plan dimensions of the slab are 4.7 x 3.2 m; supporting frame cross-sectional dimensions 200 x 240 mm; internal beams cross-sectional dimensions 100 x 160 mm; slab thickness is 60 mm. As this is a biaxial symmetrical problem, one quarter of structure was modelled applying the appertaining symmetry conditions. The structural system was point-supported as depicted in Fig. 4. Point support enables the supporting frame elements to rotate when being affected by the slab deformation and so torsion stiffness varied along the frame elements' length was taken into account. Supporting frame was thermal-isolated and so only the internal beams from three sides and the bottom edge of the SFRC slab were fire-loaded. Various tangential stiffness of timber-concrete coupling  $K_{TT,a}$ ,  $K_{TT,b}$  were applied. The slab was loaded by flat loading placed over a stripe 100 mm wide along the internal beam length with the value equal to the mechanical loading applied during the experiment – two concrete blocks, 950 kg heavy each. The appertaining dead-weight was applied too.

## Materials simulation

For timber material SOLID 3D elements were used, for SFRC material SHELL 3D elements were used. SHELL 3D elements is a specific definition offered by software Atena Science (Pryl and Červenka 2014, Červenka et al. 2014a, b), whilst these elements are numerically defined as shells but may be connected to SOLID 3D elements which enables many specific operations to be applied. The material definition, together with the loading position and the main model dimensions, can be seen Fig. 4.

**Material A** represents the real **timber frame** material – GL36c; element type – SOLID 3D Elastic; Young's modulus of elasticity  $E = 11.22$  GPa; material properties not decreased in temperature;  $\nu = 0.2$ ; coefficient of thermal expansion left constant  $\alpha = 0^\circ\text{C}^{-1}$ .

**Material B** represents the real **internal beam timber** material – GL36c; element type – SOLID 3D; specified material properties controlled in time; Young's modulus of elasticity for 25°C  $E_{(25)} = 11.22$  GPa; cross-sectional dimensions are not varied in temperature, instead an effective Young's modulus of elasticity  $E_{\text{eff}(t)}$  is applied according to formula (2) for temperature 25 through 300°C; for temperature above 300°C  $E_{(>300)} = 50$  MPa;  $\nu \rightarrow 0.0$ ; coefficient of thermal expansion left constant  $\alpha = 0^\circ\text{C}^{-1}$ .

$$E_{\text{eff}}(t) = \frac{E_{(25)} \times \frac{1}{12} (b - 2 \times \beta_0 \times t) \times (h - \beta_0 \times t)^2}{\frac{1}{12} b \times h^3} \quad (2)$$

where:  $E_{\text{eff}}(t)$  - effective Young's modulus of elasticity in time of fire,  
 $E_{(25)}$  - Young's modulus of elasticity at ambient temperature,  
 $t$  - time of fire,  
 $\beta_0$  - charring rate,  
 $b$  - width of beam,  
 $h$  - height of beam.

For the effective Young's modulus of elasticity of timber applied in the calculation see Fig. 5. In time 40 minutes the beams' collapse is considered as shown in Fig. 5.

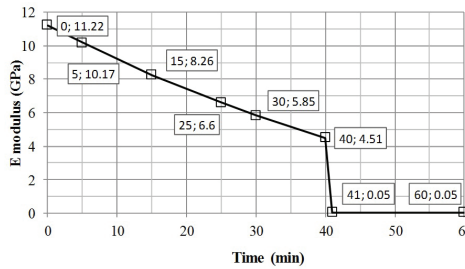


Fig. 5: Young's modulus of elasticity of internal timber beams and its variation in time.

**Material C** represents the real **SFRC material** – element type SHELL 3D temperature dependant with 8 layers in thickness (8 integration points) – non-linear element geometry – non-linear crack behaviour material. The material behaviour is a function of temperature, whilst the particular values were decreased / increased following the standard specifications and material test results (Ekr et al. 2015), up to temperature 850°C. Concrete loses its dead-weight in elevated temperatures due to water loss; therefore, based on formula (3), dead-weight was defined and considered in the numerical model:

$$\rho_{c,\theta} = \rho_{c,20} \left( 0.95 - 0.07 \times \frac{\theta - 400}{800} \right) \quad \text{for} \quad 400^\circ\text{C} < \theta_c \leq 1200^\circ\text{C} \quad (3)$$

**Material D** represents the real **SFRC material**; element type – SOLID 3D Elastic with 8 layers in thickness (8 integration points); Young's modulus of elasticity  $E = 11.22$  GPa; material properties not decreased in temperature;  $\nu = 0.2$ ; coefficient of thermal expansion left constant  $\alpha = 0^\circ\text{C}^{-1}$ .

## RESULTS AND DISCUSSION

Numerical modelling is priory focused on the global structural behaviour -the maximal vertical deflection of the coupled timber-SFRC system, and the major cracks opening pattern. Two impartial experiments were performed in 2012 and 2013, results from both of them were used to validate the numerical model. The slab behaviour can be divided into three main sections, as depicted in Fig. 6.

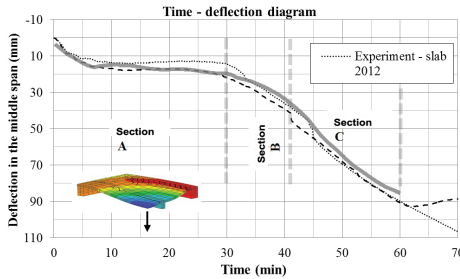


Fig. 6: Time – deflection diagram – experiment vs. model.

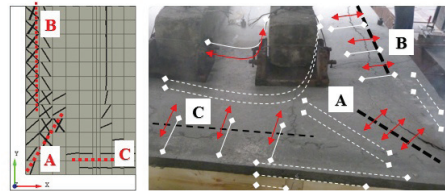


Fig. 7: Crack-opening pattern on the top edge of the slab in time 60 min. – numerical model (left), experiment (right).

The results depicted in the previous chapter are discussed furthermore in this chapter.

**Section A** is characteristic for its initial deflection in the first 5 to 10 min. of the experiment. In this section, the initial material properties definition and also the coupling tangential stiffness need to be defined properly to reach the results comparable with the experimental ones. Rapid deflection is caused by several factors. First of all, rapid temperature increase based on the applied fire curve, when temperature increases from 25 to 700°C within the first 10 minutes. This causes rapid changes mainly in the structure of timber which loses its E modulus (Wald et al. 2005, ČSN EN 1995-1-2 2006) without being self-protected by the charring layer yet (Reinprecht 2008). Another factor is the heat capacity of concrete – even when being under fire loading, the material temperature is rather low – based on both the thermal simulation and the experimental results, the temperature of concrete 20 mm above the bottom edge is  $T_{(10\text{min.})} \approx 100^\circ\text{C}$ , whilst  $T_{(60\text{min.})} \approx 540^\circ\text{C}$ , see also (Ekr et al. 2015). Due to this, thermal strains on the bottom edge reach only low values and so an effect of the bottom edge being elongated and so rotate the support frame outwards the slab span is not dominant in the very first phase of the experiment.

The following stage is represented by the time-deflection curve and its horizontal shape in time from 10 to 30 min. In this phase, primary load-bearing timber beams lose their bending stiffness under the effects of timber being thermal degraded, slab material mechanical properties are also thermal degraded and thermal strains reach higher values. As all these principal phenomena are balanced all the time during this phase, a horizontal time-deflection curve can be observed.

**Section B** is characterized by the internal beams gradual failure. As the beams lose the bending stiffness, the vertical deflection increases and elongation of the bottom beam edge is followed by “timber spalling”. Charred layers of burned timber are taken off the beam’s surface which was clearly observed during the experiment. Due to this action, timber is not self-protected, as assumed previously, but thermal not-degraded layers become exposed to fire. Gradual increase of vertical deflections results into the internal forces redistribution.

**Section C** is characterized by a gradual increment of the slab deflection after a complete failure of the internal beams. Gradual cracking of timber beams was observed, up to the failure of one of them, which was followed by a failure of another one in a short time. This moment can be observed in both experimental time-deflection curves depicted in Fig. 6 as a rapid increment of deflection with value equal to approx. 5 mm.

In this section, either a collapse or a membrane action occurrence was expected. Since a collapse was not observed, membrane forces are expected to occur. The coupled timber-SFRC



load-bearing system is primarily bended at ambient temperature. In this phase, simply a beam action may be considered when designing such system. However, in elevated temperature, without internal beams and due to loss of strength of the subjected slab, deformation of the thin slab increases and so tensile membrane action may occur. Planar stiffness of the slab is much higher than its bending stiffness, see also (Stadler 2012). As a membrane action itself cannot be measured *in situ*, vertical displacements and crack-opening patterns were directly observed and consequently used to propose the final conclusions. This observation was performed in compliance with the following quotation:

“It doesn't matter how beautiful your theory is, it doesn't matter how smart you are. If it doesn't agree with experiment, it's wrong”. Richard P. Feynman (1918 – 1988), holder of Nobel Prize in Physics (1965)

Especially in this case, observing the crack-opening pattern helps to understand the specific behaviour of a structure. As the energy equilibrium is in balance each time during an experiment and the material properties being continuously varied due to high temperature, the static scheme and loading transfer varies in time too. These changes can be clearly distinguished by the crack-opening pattern variation during the experiment.

Crack-opening pattern in time 60 min. resulted from the numerical model compared with the experiment is depicted in Fig. 7.

Numerical simulation proves the cracks opening across the slab thickness – both in the bottom and the top surface in areas marked as ‘A’ and ‘B’ in Fig. 7. The same phenomena was observed during the experiment, see also (Caldová et al. 2014b), where the slab lost its integrity locally in the marked areas. In an area marked as ‘C’, only top surface cracks opened, which was also proved both by the numerical simulation and real-size experiment. Integrity of the subjected slab was locally corrupted, however, the structure disposed of residual resistance and did not collapse even after being exposed to 60 min. of nominal fire actions. Based on the observed cracks pattern and numerical simulation results, a stress-pattern is depicted in Fig. 7. When a couple of curves/lines is plotted, the top one represents top edge stresses direction; the bottom one represents bottom edge stresses direction; an arrow is for tension, a square is for compression; dashed line is for stresses across the slab thickness. As the slab corner is restrained from being lifted up, there are also stresses in the “z” direction present, however, not plotted.

## CONCLUSIONS

Observed serviceability and integrity time of both the slabs exceeded the standard ones, which was also proved by the numerical simulations.

Coupling timber-concrete was observed during the beams life time – service time.

Large deflections and vertical support system enabled the tensile membrane forces to occur.

Cooperation of unprotected timber beams and a thin fibre-concrete slab is effective in fire conditions and helps to improve fire resistance of a subjected load bearing system.

Numerical models with standard input data can be used to analyse scenarios as presented in this paper, however, material non-linearity, geometric non-linearity, time and temperature dependence of material properties needs to be taken into account.

Fire resistance of unprotected timber beams may be increased without using any additional fire isolation – this is the subject matter of the following research at ČVUT in Prague.

## ACKNOWLEDGMENTS

This publication was supported by the European social fund within the framework of realizing the project „Support of inter-sectoral mobility and quality enhancement of research teams at Czech Technical University in Prague“, CZ.1.07/2.3.00/30.0034. Period of the project's realization 1.12.2012 – 30.6.2015. Project was also supported by grant GAČR 15-19073S.

## REFERENCES

1. Barros, J.A.O., Sena Cruz, J., 2001: Fracture energy of steel fibre reinforced concrete. *Mechanics of Composite Materials and Structure* 8(1): 29-45. DOI: 10.1080/10759410119428.
2. Bednář, J., Wald, F., Vodička, J., Kohoutková, A., 2013: Experiments on membrane action of composite floors with steel fibre reinforced concrete slab exposed to fire. *Fire Safety Journal* 59(6): 111-121. DOI: 10.1016/j.firesaf.2013.04.008.
3. Blesák, L., Goremikins, V., Wald, F., Sajdlová, T., 2015: Material model of steel fibre reinforced concrete subjected to high temperatures. *Fire Safety Journal*. Being reviewed.
4. Caldová, E., Blesák, L., Wald, F., Kloiber, M., Urushadze, S., 2014a: Behaviour of timber and steel fibre reinforced concrete composite constrictions with screwed connections. *Wood Research* 59(4): 639-660.
5. Caldová, E., Vymlátíl, P., Wald, F., Kuklíková, A., 2014b: Timber steel fibre-reinforced concrete floor slabs in fire: Experimental and numerical modelling. *Journal of Structural Engineering* DOI: 10.1061/(ASCE)ST.1943-541X.0001182.
6. Červenka, V., Červenka, J., Janda, Z., Pryl, D., 2014a: ATENA program documentation. Part 8. User's manual for ATENA-GiD. Interface, Červenka Consulting Ltd, 115 pp.
7. Červenka, V., Jendele, L., Červenka, J., 2014b: ATENA program documentation. Part 1. Theory. Červenka Consulting Ltd, 290 pp.
8. ČSN EN 1995-1-2, 2006: Design of timber structures – Part 1-2: General – Structural fire design.
9. Ekr, J., Caldová, E., Vymlátíl, P., Wald, F., 2015: Design model for timber steel fibre reinforced concrete floor slabs. *Journal of Structural Engineering* (under preparation).
10. Elsaigh, W.A., 2001: Steel fibre reinforced concrete ground slabs. A comparative evaluation of plain and steel fibre reinforced concrete ground slabs. Master thesis, University of Pretoria.
11. Pryl, D., Červenka, J., 2014: ATENA program documentation. Part 11. Troubleshooting manual. Červenka Consulting Ltd, 58 pp.
12. Reinprecht, L., 2008: Wood protection. University handbook, Technical University in Zvolen, 453 pp (in Slovak).
13. Sajdlová, T., 2011: Steel fibre reinforced concrete – Material model parameters definition based on experimental results. Published by Czech Technical University in Prague.
14. Salehian, H., Barros, J.A.O., Taheri, M., 2014: Evaluation of the influence of post-cracking response of steel fibre-reinforced concrete (SFRC) on load carrying capacity of SFRC panels. *Construction and Building Materials* 73: 289-304.
15. Sandanus, J., 2007: Parametric study of the factors affecting the resistance of a composite timber-concrete cross-section. *Wood Research* 52(3): 109-114.
16. Stadler, M., 2012: Design of composite slab systems in case of fire using simplified finite element analyses. Doctoral thesis, Technical University in Munich, 141 pp.

17. Wald, F., Burgess, I., De La Quintana, J., Vila Real, P., 2005: Calculation of fire resistance of building structures. Published by Czech Technical University in Prague, ISBN 80-01-03157-8, 239 pp.

LUKÁŠ BLESÁK \*, EVA CALDOVÁ, FRANTIŠEK WALD  
CZECH TECHNICAL UNIVERSITY IN PRAGUE  
DEPARTMENT OF STEEL AND TIMBER STRUCTURES  
THÁKUROVA 7  
PRAGUE CZ16629  
CZECH REPUBLIC  
PHONE: +421 776 251 353  
Corresponding author: lukas.blesak@fsv.cvut.cz

